




# The tempo of greening in the European Alps: Spatial variations on a common theme

Philippe Choler<sup>1</sup>  | Arthur Bayle<sup>1</sup>  | Bradley Z. Carlson<sup>2</sup>  | Christophe Randin<sup>3</sup>  | Gianluca Filippa<sup>4</sup>  | Edoardo Cremonese<sup>4</sup> 

<sup>1</sup>Univ. Grenoble Alpes, Univ. Savoie Mont Blanc, CNRS, LECA, Grenoble, France

<sup>2</sup>Centre de Recherches sur les Écosystèmes d'Altitude (CREA), Chamonix, France

<sup>3</sup>Department of Ecology & Evolution/ Interdisciplinary Centre for Mountain Research (CIRM), Université de Lausanne, Lausanne, Switzerland

<sup>4</sup>Climate Change Unit, Environmental Protection Agency of Aosta Valley, Saint-Christophe, Italy

## Correspondence

Philippe Choler, Univ. Grenoble Alpes, Univ. Savoie Mont Blanc, CNRS, LECA, F-38000 Grenoble, France.  
Email: philippe.choler@univ-grenoble-alpes.fr

## Funding information

Région Auvergne-Rhône-Alpes, Grant/Award Number: CPER07\_13 CIRA; Agence Nationale de la Recherche, Grant/Award Number: ANR10 LABX56 and ANR-10-EQPX-29-01; LIFE PASTORALP Project, Grant/Award Number: LIFE16 CCA/IT/000060; Interreg ALCOTRA CCLimaTT

## Abstract

The long-term increase in satellite-based proxies of vegetation cover is a well-documented response of seasonally snow-covered ecosystems to climate warming. However, observed greening trends are far from uniform, and substantial uncertainty remains concerning the underlying causes of this spatial variability. Here, we processed surface reflectance of the moderate resolution imaging spectroradiometer (MODIS) to investigate trends and drivers of changes in the annual peak values of the Normalized Difference Vegetation Index (NDVI). Our study focuses on above-treeline ecosystems in the European Alps. NDVI changes in these ecosystems are highly sensitive to land cover and biomass changes and are marginally affected by anthropogenic disturbances. We observed widespread greening for the 2000–2020 period, a pattern that is consistent with the overall increase in summer temperature. At the local scale, the spatial variability of greening was mainly due to the preferential response of north-facing slopes between 1900 and 2400 m. Using high-resolution imagery, we noticed that the presence of screes and outcrops locally magnified this response. At the regional scale, we identified hotspots of greening where vegetation cover is sparser than expected given the elevation and exposure. Most of these hotspots experienced delayed snow melt and green-up dates in recent years. We conclude that the ongoing greening in the Alps primarily reflects the high responsiveness of sparsely vegetated ecosystems that are able to benefit the most from temperature and water-related habitat amelioration above treeline.

## KEYWORDS

climate change, European Alps, greening, mountain ecosystems, NDVI, remote sensing

## 1 | INTRODUCTION

The long-term increase in greenness in cold, seasonally snow-covered ecosystems is widely perceived as a consequence of climate change (Berner et al., 2020; Keenan & Riley, 2018). Arctic and alpine ecosystems have undergone particularly fast greening compared to other ecosystems and this is consistent with the accelerated warming documented for these regions (Callaghan et al., 2010; Pepin et al., 2015). However, this greening exhibits considerable spatial

and temporal variability that is far from being understood (Berner et al., 2020; Cortés et al., 2021; Ju & Masek, 2016; Myers-Smith et al., 2020). The complex interaction between regional climate trends, topography, geomorphological and other disturbance regimes and vegetation dynamics contributes to these non-uniform patterns of greening (Ropars & Boudreau, 2012; Tape et al., 2012). Further studies are required to document the relative contribution of these drivers and to advance a more predictive understanding of greening and its consequences on ecosystem processes and services

(Duveiller et al., 2018; Forzieri et al., 2017; Myers-Smith et al., 2020; Zhu et al., 2016).

Temperate mountains have experienced warmer summers over the last decades (Beniston, 2006; Hock et al., 2019). Several studies have underlined the impact of these changes on land surface phenology (Asam et al., 2018; Dunn & de Beurs, 2011; Xie et al., 2020; Zhang et al., 2013), ecosystem productivity (Choler, 2015; Jolly et al., 2005) and species richness (Lamprecht et al., 2018; Steinbauer et al., 2018). Other studies reported on the long-term increase in greenness in the south-western Alps (Carlson et al., 2017; Filippa et al., 2019), the Hindu Kush (Anderson et al., 2020) and underlined the particular responsiveness of sparsely vegetated areas located in the nival belt. However, none of these studies has provided a comprehensive analysis of the spatial variability of greening at the mountain range scale and an investigation of its determinants. More specifically, the distinction between exposure to change (e.g. climate) and the responsiveness of ecosystems to change has remained elusive. Yet, well-documented case studies in the Arctic suggest that this fundamental question may underpin much of the observed spatial complexity of greening. For example, the preferential expansion of arctic shrubs in particular topographical situations, such as along streams or in floodplains, led to local-scale greening heterogeneity (Tape et al., 2006), which in turn is possibly related to the snow-holding capacity of shrubs in winter (Sturm et al., 2005). The initial cover of *Betula glandulosa* in the 1950s explained part of the spatial variability of greening in Nunavik (Ropars & Boudreau, 2012; Ropars et al., 2015). These studies pointed out that land cover properties are pivotal to predict the responsiveness of the system to ongoing changes and to identify the underlying ecological mechanisms of greening.

There is a growing body of evidence showing that mountain ecosystems of the Alps have undergone rapid changes in response to climate warming (Gottfried et al., 2012). Plot-based long-term surveys revealed increasing vegetation cover in mountain grasslands, mainly due to the expansion of graminoids (Rogora et al., 2018) and a colonization of screes and outcrops by shrubs and trees (Vittoz, Bodin, et al., 2008). While these studies are invaluable to inform on ecological mechanisms underpinning ecological changes, their paucity precludes tracking complex, non-linear responses along topographical, geomorphological and climate gradients. For example, winter snow duration—which is widely acknowledged as a key driver of vegetation dynamics—for the time being shows decreased sensitivity to global warming at elevations above 2000 m (Hantel & Hirtl-Wielke, 2007; Schoener et al., 2019). Another issue is the over-representation of high summits in plot-based surveys, considering that the area they cover represents a minute fraction of above-treeline habitats. For these reasons, remote sensing offers a complementary approach to probe ongoing land cover changes at a scale encompassing multiple environmental gradients and to examine their impacts on ecosystem services such as water provisioning, carbon sequestration or pastoral resources.

Here, we exploit available time series of the moderate resolution imaging spectroradiometer (MODIS) to provide a comprehensive

picture of recent greening and its spatial variability in the European Alps and to improve our understanding of its drivers. Our study utilizes annual peak values of the Normalized Difference Vegetation Index (NDVI) as a proxy of land surface greenness (Tucker, 1979). We quantified the significance and magnitude of NDVI trends for high-elevation ecosystems that are located between the treeline and the permanent snowline. This allows us to overcome two potential issues in such remote sensing studies. First, high-elevation ecosystems are less affected by anthropogenic disturbances than other European habitats at lower elevation, which should facilitate the unravelling of a climate signal on greening trends (Filippa et al., 2019; Gehrig-Fasel et al., 2007). Second, the NDVI range of these ecosystems lies in a range where it is highly sensitive to land cover and biomass changes, in contrast to closed canopies where NDVI no longer linearly depends on biomass or plant cover (Huete et al., 2002; Myneni & Williams, 1994).

We addressed the three following questions:

1. How widespread is the greening signal in above-treeline ecosystems of the European Alps?
2. Is the variability of greening spatially structured and what are its main drivers?
3. Are there fine-scale land cover features that predispose to fast greening response?

## 2 | MATERIAL AND METHODS

### 2.1 | Study area and selection of pixels

The European Alps stretch over 1200 km from Nice (France) to Vienna (Austria). Our study focuses on the uplands of the massif that are located between the treeline and the permanent snowline. This area includes shrublands, grasslands and sparsely vegetated ecosystems established on screes, debris and outcrops. We first selected a set of 250-m resolution MODIS pixels having non-forested land cover classes with a tree cover density below 5%, an elevation above 1400 m and an average  $NDVI_{max}$  above 0.15. To do so, we relied on a 25-m resolution Digital Elevation Model, a 100-m resolution Tree Cover Density map for the year 2018 (<https://land.copernicus.eu/pan-european/high-resolution-layers/forests/tree-cover-density/>) and the Corine Land Cover (CLC) product for 2018 (<https://land.copernicus.eu/pan-european/corine-land-cover/>), which is based on the visual photointerpretation of aerial images at a 100-m resolution. From the 44 CLC entries at level 3, we retained the following classes: Pastures (code 2.3.1), Natural grasslands (code 3.2.1), Moors and heathlands (code 3.2.2), Bare Rocks (code 3.3.2) and Sparsely vegetated (code 3.3.3). We merged pastures and grasslands, and we renamed the misleading 'bare rocks' to 'very sparsely vegetated' as we selected pixels with an average  $NDVI_{max}$  above 0.15, that were not completely devoid of vegetation. We discarded pixels exhibiting more than 10% of settlements (ski resorts) or permanent water using data layers of European settlements (<https://land.copernicus.eu/pan-european/high-resolution-layers/settlements/>).

eu/pan-european/GHSL/european-settlement-map/) and of permanent water (<https://land.copernicus.eu/pan-european/high-resolution-layers/water-wetness/status-maps/water-wetness-2018>). We also removed pixels for which we found significant abrupt changes of  $NDVI_{max}$  within the period 2000–2020, as this might be indicative of a physical or anthropogenic disturbance unrelated to climate trend. This was done by using the Breaks For Additive Seasonal and Trend (BFAST) on 8-day NDVI time series. Breaks were identified after the time-series decomposition into trend, seasonal and remainder component. Abrupt changes were considered as break points when their uncertainty was found to be smaller than 1 year, consistent to a previous study in the south-western Alps (Filippa et al., 2019). This led to discard around 5% of the total number of pixels. We ended up with 511,375 pixels of which 284,346 (55.6%) exhibited an average  $NDVI_{max}$  below 0.65. Our main findings are based on this data subset to avoid the saturation effect of  $NDVI_{max}$  for closed canopies (see Section 1; Figure S2). Figure S3 and Table S1 give the spatial distribution of these pixels and their breakdown by administrative units using the Nomenclature of territorial units for statistics (NUTS) classification at level 3 (<https://ec.europa.eu/eurostat/web/gisco/geodata/reference-data/administrative-units-statistical-units/>). Figure S12 shows the distribution of pixels for elevation and diurnal anisotropic heating (DAH) classes. We processed all spatial data using the *raster*, *rgdal*, *sp* and *proj4* R packages (Venables & Ripley, 2002). We used the *bfast* R package to implement the BFAST analysis (Verbesselt et al., 2010).

## 2.2 | Estimates of MODIS-derived NDVI metrics

We downloaded the 250-m resolution 8-day composite of MOD09Q1/Terra collection 6 products that are available in hdf format at the Land Processes Distributed Active Archive Center (<https://e4ftl01.cr.usgs.gov/>). Acquired dates covered the period from 18 February 2000 to 27 December 2020. We assembled the tiles h18.v4 and h19.v04 in order to cover the entire massif and re-projected red and near-infrared (NIR) surface reflectance values ( $\rho$ ) in the EPSG 3035 geometry. We retained reflectance values produced with high quality (according to the MOD09Q1 Quality Control flag) and calculated a NDVI according to  $(\rho_{NIR} - \rho_{RED}) / (\rho_{NIR} + \rho_{RED})$ , where  $\rho$  is the reflectance. We did not use the 500-m-resolution 16-day composite BRDF-corrected MODIS products (MCD43A4) as we needed a higher temporal and spatial resolution to best capture changes in peak NDVI during the short growing season above treeline. Raw NDVI time series were processed in two steps. First, we used the Best Index Slope Extraction algorithm to reduce the noise of the NDVI time series (Viovy et al., 1992) with the parameters:  $n = 0.2$  (i.e. a 20% acceptable difference in NDVI values within the sliding period) and  $p = 3$  (the length of the forward sliding period). Second, we applied a low-pass filter using the Savitzky–Golay algorithm (Savitzky & Golay, 1964) with the following parameters:  $n = 3$  (the filter order) and  $p = 7$  (the filter length). Smaller values of  $p$  would allow keeping track of more rapid changes, whereas higher

values would increase the smoothing. We also estimated a green-up date as the first date of the year where the NDVI reached 50% of the  $NDVI_{max}$ . This was achieved using daily-interpolated time series of NDVI. Green-up date is highly correlated with snow melt-out timing in the high-elevation mountain grasslands of the Alps (Choler, 2015; Fontana et al., 2008). We used the non-parametric, rank based, Mann–Kendall (MK) monotonic test to assess the significance of NDVI time-series trends. The significance was given by the approximately normally distributed z score with z values  $> 1.96$  indicating a significant increase ( $p < .05$ ) and z values  $< -1.96$  a significant decrease (at  $p < .05$ ). To quantify change over the period 2000–2020, we fitted linear models based on Theil–Sen single median slope. The Theil–Sen estimator of the linear trend is much less sensitive to outliers than the least squares estimator. The distribution of  $NDVI_{max}$  slopes for the different ranges of  $NDVI_{max}$  values is shown in Figure S2. Decreasing slope values in the highest ranges of  $NDVI_{max}$  were clearly indicative of a saturation effect. For further analyses, we retained pixels with an  $NDVI_{max}$  value between 0.15 and 0.65. In this range, the pairwise mean difference of greenness slopes was below 0.005 (Figure S2). We randomly perturbed the RED and NIR raw reflectance by up to  $\pm 5\%$  to and recalculated 1000 times the MK trends and the Theil–Sen slopes for all pixels. The uncertainty of MODIS reflectance, and therefore of vegetation indices, arises from sensor calibration and the different steps of atmospheric correction (Vermote & Vermeulen, 1999). A perturbation of 5% lies in the upper range of the uncertainties associated with MODIS products (Miura et al., 2000). Our numerical simulation propagates this uncertainty into the estimates of NDVI trends and ensures a more robust analysis of the drivers of greening using random forest. We used the *Kendall* R package for estimating MK trends (McLeod, 2005) and the *signal* R package for the Savitzky–Golay function (Signal Developers, 2013).

## 2.3 | Preparation of predictor data sets

We estimated terrain indices from the 25-m resolution European Digital Elevation Model (EU-DEM, version 1.0; <https://land.copernicus.eu/imagery-in-situ/eu-dem/>). We resampled the EU-DEM to 250-m resolution and calculated the mean, range and standard deviation of elevation and the DAH. The DAH index approximates the anisotropic heating of land surface to radiation (Böhner & Antonić, 2009). We computed DAH as  $\cos(\alpha_{max} - \alpha) \arctan(\beta)$ , where  $\alpha$  is the aspect,  $\beta$  is the slope and the parameter  $\alpha_{max}$  corresponds to the aspect with the maximum total heat surplus. We used  $\alpha_{max} = 212^\circ$  as we noticed that this SSW orientation corresponds on average to the earliest first snow-free day derived from Sentinel-2 products in the south-western Alps (unpublished results). Bedrock data were extracted from the 1:1 million OneGeology pan-European harmonized surface geological maps distributed by the European Geological Data Infrastructure portal (<http://www.europe-geology.eu/>). Surface geological units were aggregated into four categories: (i) igneous and metamorphic rocks including granite, gneiss etc.; (ii) ferromagnesian rocks including serpentines, amphibolite, andesite, basalt etc.; (iii)

hard sedimentary rocks including dolomite, limestone etc; and (iv) clastic sedimentary rocks including schist, mudstone, shale, flysch etc. For climate trends, we used the daily-based gridded data sets of E-OBS at a 0.1° resolution for the period 1995 onwards (version E-OBS v22.0e; [https://surfobs.climate.copernicus.eu/dataaccess/access\\_eobs.php](https://surfobs.climate.copernicus.eu/dataaccess/access_eobs.php)) (Cornes et al., 2018). For each year, we calculated growing degree days (GDD) as the cumulative sum of daily average air temperature above 0°C during the summer months (June, July and August). As a complementary estimate of summer warming, we also extracted the average of daily maximum temperatures in July (T07). We computed a climatic water balance as the difference between precipitation ( $P$ ) and a reference crop evapotranspiration  $ET_0$ . We summed the  $P-ET_0$  difference over the summer months to assess the dry-wet conditions of the growing season.  $ET_0$  was estimated on a daily basis using the equation  $\lambda ET_0 = C (\Delta/\Delta + \gamma) Q$ , where  $Q$  is the global radiation ( $\text{MJ m}^{-2} \text{day}^{-1}$ ),  $\Delta$  is the slope of the vapour pressure-temperature curve ( $\text{kPa}^\circ\text{C}^{-1}$ ),  $\gamma$  is the psychrometric constant ( $\text{kPa}^\circ\text{C}^{-1}$ ),  $\lambda$  is the latent heat of vaporization ( $\text{MJ kg}^{-1}$ ) and  $C$  is an empirical coefficient ( $C = 0.65$ ). This is a simplified version of the Penman-Monteith equation originally proposed by Makkink and later modified by Hansen (1984). Maps of climate predictors are shown in Figures S9 and S10. For snow cover duration trends in the French Alps (Figure S11), we used the S2M meteorological and snow cover re-analysis for the period 1959–2019 (<https://www.aeris-data.fr/catalogue/>; Vernay et al., 2019). As for NDVI time series, we used the non-parametric MK monotonic test and the Theil-Sen median slope to assess the significance and the magnitude of decadal trends for all meteorological variables.

### 2.3.1 | Random forest analysis

We implemented a random forest analysis to identify the best predictors of the spatial variability of greening. Based on the MK significance tests, we classified the greenness trends into the following three categories: no significant greening ( $p > .005$ ), moderate greening ( $.005 < p < .05$ ) and strong greening ( $p < .005$ ). There were not enough pixels exhibiting browning to include this response in the analysis. We randomly sampled 15,000 pixels in each category to balance the sample size among the greening responses and partitioned the data set into a model training subset (two thirds of pixels) and a model evaluation subset (one third of pixels). We repeated this procedure 1000 times, meaning that we assembled one random data set for each perturbed simulation of MODIS reflectance and implemented one random forest model for each data set. Predictor variables included elevation, DAH, bedrock,  $\text{NDVI}_{\text{max}}$  anomaly and decadal trends for the green-up date, and the climate variables included GDD and  $P-ET_0$ . We calculated pairwise correlations between predictors and checked that they were not highly correlated, that is  $r < .5$  (Figure S13). We also implemented a random forest model including  $\text{NDVI}_{\text{max}}$  to check for its influence on the classification probability and to further document the saturation effect (Figure S6). We relied on the out-of-bag classification accuracy to select the best

random forest model. We assessed predictor importance using the mean decrease in accuracy metric, which is indicative of the suitability of a predictor, and the mean decrease in Gini, which is indicative of the homogeneity of nodes and leaves. Predictor importance was based on a permutation-based importance measure, where one measures the effect of reshuffling each predictor on model accuracy. Last, we examined how classification probabilities depend on the values taken by each predictor by computing partial dependence plots. We computed empirical cumulative distribution function to determine the range of values where interpretation of partial dependence plots needs caution due to small sample size. We used the *randomForest*, *caret* and *pdp* R packages to implement random forest models and evaluate their performance (Greenwell, 2017; Kuhn, 2020; Liaw & Wiener, 2002).

### 2.3.2 | Land cover assessment using very high-resolution imagery

Using the high-resolution imagery of Google Earth, we characterized the land cover features of a selection of 300 500 × 500 m cells. First, we aggregated  $\text{NDVI}_{\text{max}}$  anomaly at a 500-m resolution. Then we performed a stratified random sampling of pixels using three classes of  $\text{NDVI}_{\text{max}}$  anomaly—negative, around zero and positive values—and 100 pixels in each class (Figure S7). The visual photointerpretation of very high-resolution imagery from Google Earth allows us to distinguish the following six types of object: singular trees or tree patches, tall shrubs or shrublands (mainly composed of *Pinus mugo*), low shrublands (presumably *Ericaceae*-dominated), grasslands, screes and debris and finally outcrops. We assigned a percentage cover to these classes using the semi-quantitative ranges: <5%, 5%–25%, 25%–50%, 50%–75% and 75%–100%. Three authors of this study (PC, EC and GF) conducted the photointerpretation independently and we retained the most frequent cover estimate for each land cover class. We did not try to standardize the year of satellite view, as there were no sufficient good quality images to do it.

## 3 | RESULTS

Over the 2000–2020 period, we found significant ( $p < .05$ ) positive temporal trends in  $\text{NDVI}_{\text{max}}$  for 56% of the 284,346 analysed pixels and significant negative trends for <0.1% of all pixels (Figure 1a; Table S1). Irrespective of significance, the ratio between positive and negative slopes was 26/1. These results were robust to uncertainty in MODIS data, as more than two thirds of the pixels classified as fast ( $p < .005$ ) and non-significant greening ( $p > .05$ ) remained in these two classes when reflectance values were randomly perturbed (Figure S1). Sparse and very sparse vegetation contributed to 23% and 26%, respectively, of the 56% of significant greening compared to 7% for grasslands and heathlands (Figure 1b). Figure S2 shows that there was no strong effect of the average  $\text{NDVI}_{\text{max}}$  on the magnitude of greening in the selected range (0.15–0.65). By

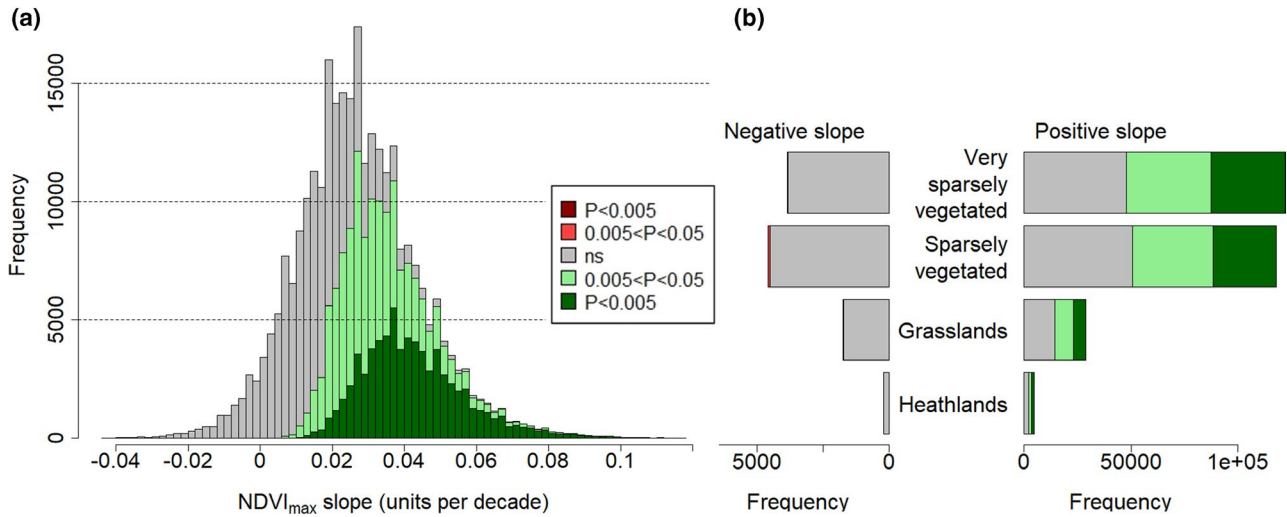


**FIGURE 1** Sign and magnitude of greenness trends in above-treeline ecosystems of European Alps. (a) Frequency distribution of linear trends in  $NDVI_{max}$  for the 2000–2020 period. Slopes were estimated using the Theil–Sen median slope analysis. Levels of significance were assessed by a non-parametric, rank based, Mann–Kendall monotonic test. Positive values correspond to greening, while negative values represent browning trends. The analysis was performed on 284,546 pixels at 250-m resolution. (b) Greenness trends by land cover class, based on the European-scale product Corine Land Cover (CLC). Note that the CLC class ‘bare rocks’ was renamed ‘very sparsely vegetated’ as the average  $NDVI_{max}$  of selected pixels was above 0.15. Note the highly contrasting scale for positive and negative trends.  $NDVI$ , Normalized Difference Vegetation Index

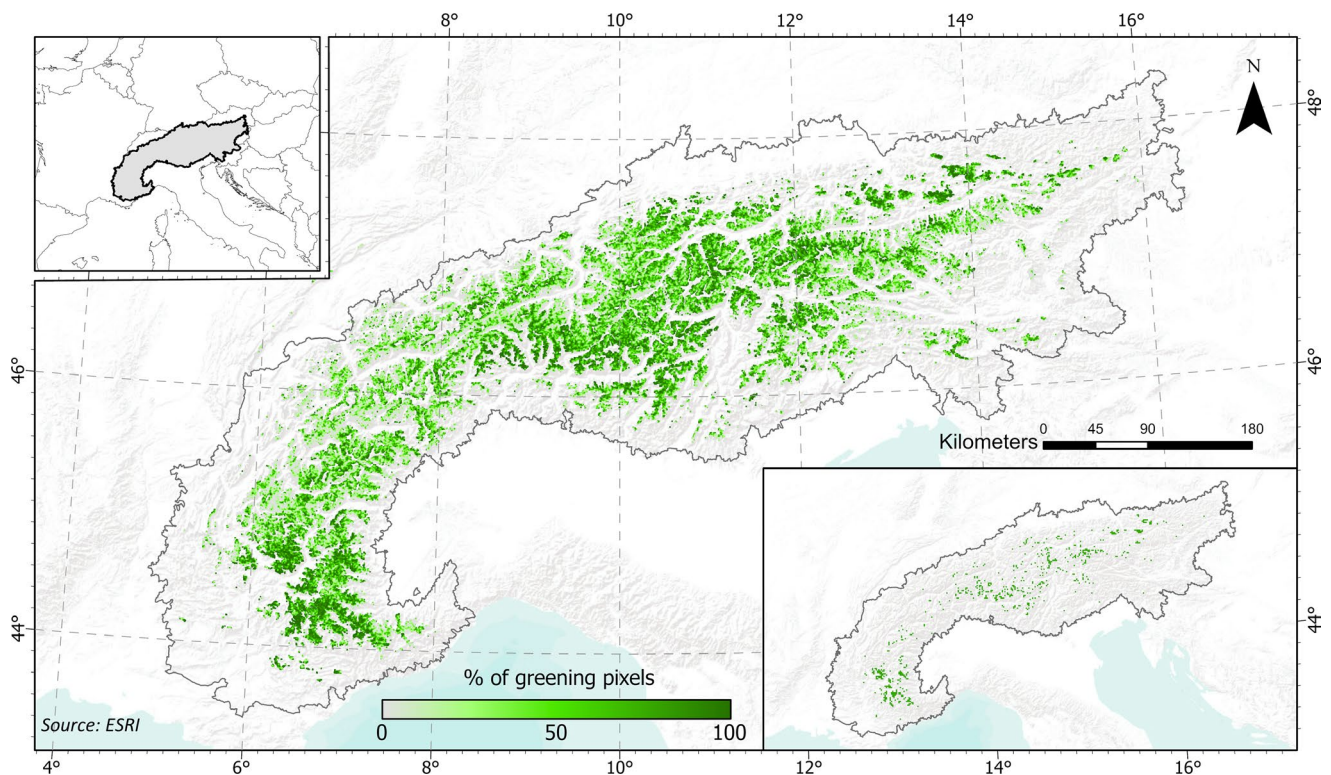


**FIGURE 2** Spatial distribution of greenness trends. For visual clarity, we applied a  $5 \times 5$  pixels moving window to the original 250-m resolution map. The colour scale represents the percentage of pixels showing significant greening ( $p < .05$ ) over the 2000–2020 period. The bold line indicates the boundaries of the European Alps, whose general location is shown in the upper left insert. The lower right insert highlights regional hotspots of greening by aggregating the 250-m resolution map to 2.75 km and by colouring pixels for which more than 80% of the 250-m pixels exhibited fast greening ( $p < .005$ )

contrast, there was a marked decline in greening for higher values of  $NDVI_{max}$  suggesting a saturation effect (Figure S2; Table S1). Only 31% of pixels exhibited a significant greening when the  $NDVI_{max}$  value was above 0.65 (Table S1).

Although widely distributed, the greening trends are not spatially uniform (Figure 2). We found a regional-scale component of this spatial variability, with hotspots of greening corresponding to southern parts of the French Alps (e.g. Haute-Provence and Maritime Alps, France), the southern part of the Central Alps (e.g. Sondrio, Italy and Tiroler Oberland, Austria) and the north-easternmost part of the Alps (e.g. Pinzgau-Pongau, Austria; Figure 2; Figure S3; Table S1). At the local scale, topographical factors also modulate observed greening trends (Figure 3a). First, there is a general tendency for the greening to increase with elevation (Figure 3a). Second, and on top of that, the greening is more noticeable on steep north-facing slopes, that is, for the most negative values of DAH (Figure 3a). Consequently, we observed an overall upward shift of the isolines of  $NDVI_{max}$ , meaning that the elevation of given value of  $NDVI_{max}$  has increased steadily over the last two decades (Figure 3b). We estimated the median of this shift at 45 m per decade with strong regional disparities (Figure S4). It is worth noting that the magnitude of this elevational shift is higher for the first deciles of the distribution than for the last, and this difference is particularly striking at negative DAH values (Figure 3b). These results point out that greening is enhanced when the  $NDVI_{max}$  is below the median of the distribution for a given elevation and DAH, leading to a reduction of the interdecile differences in the distribution of  $NDVI_{max}$  along topographical gradients (Figure 3b).

These findings prompted us to quantify a per-pixel  $NDVI_{max}$  anomaly and to assess its spatial distribution in the European Alps. The anomaly was calculated as the difference between the average  $NDVI_{max}$  of a given pixel and the median  $NDVI_{max}$  value of all pixels lying in the same class of DAH and elevation (Figure 4a). Negative anomalies are indicative of an 'abnormally' low  $NDVI_{max}$  value with respect to elevation and DAH. The mapping of this anomaly revealed a clear regional-scale variability that was partly congruent with that of greening (Figure 4b). For example, the southern part of the French Alps, part of the south Central Alps and the north-easternmost Alps are regions that present a combination of fast greening (Figure 2), negative  $NDVI_{max}$  anomalies (Figure 4b) and high upward shift of  $NDVI_{max}$  (Figure S4).

We evaluated the importance of this  $NDVI_{max}$  anomaly in predicting the observed greening trends against two sets of predictors that are more widely used in greening studies, that is topographical predictors (elevation and DAH) and climate predictors pertaining to the growing season (summer). We used trends in the accumulation of GDD during summer as a proxy of temperature-related changes and trends in the difference between precipitation and potential evapotranspiration as a proxy of water balance-related changes (see Section 2). We also estimated trends in the green-up date derived from the analysis of NDVI time series. Previous studies showed that the green-up date strongly depends on snow cover duration in high-elevation temperate ecosystems (Choler, 2015). We built a random forest model to assess the usefulness of these variables for classifying pixels into three categories based on the MK significance test—no greening ( $p > .05$ ), moderate greening ( $p < .05$ ) and fast

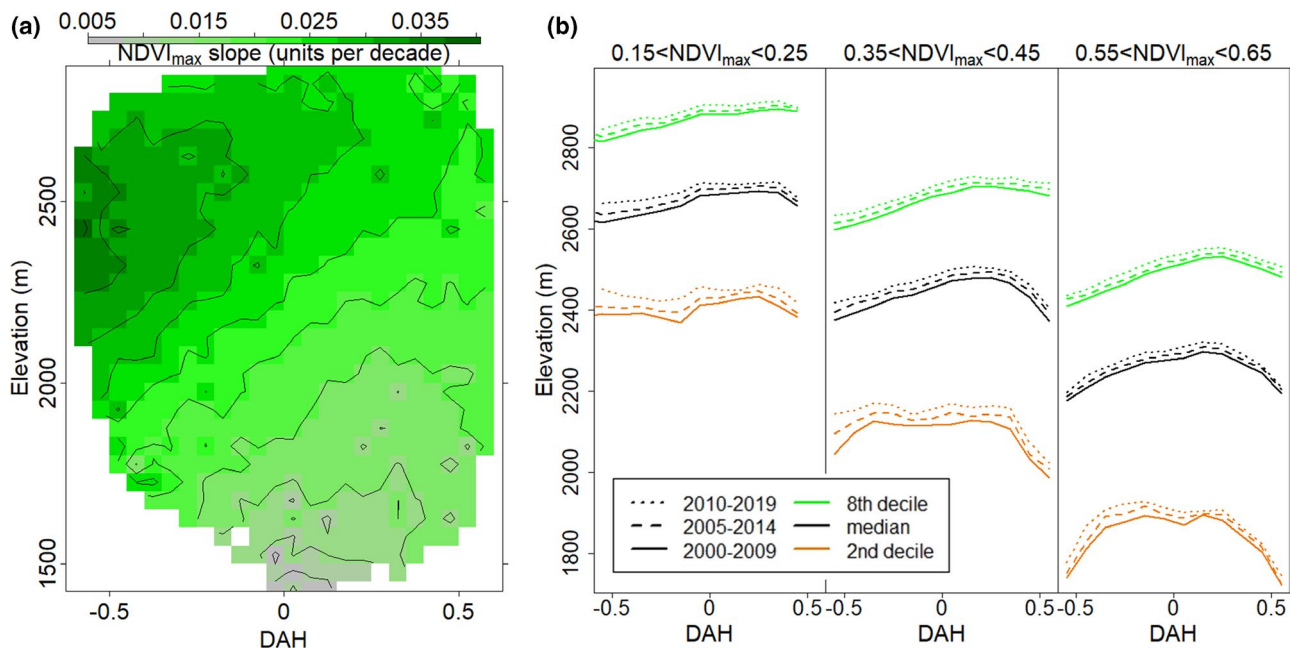


**FIGURE 3** Variation of greenness trends along gradients of elevation and diurnal anisotropic heating (DAH). (a) Heat map of the mean value of  $NDVI_{max}$  slopes per class of elevation and DAH. Only combinations representing more than 5% of the total number of pixels are shown. (b) Elevational distribution of three ranges of  $NDVI_{max}$  as a function of DAH. Lines indicate the second decile, the median and the eighth decile of the distribution. Average  $NDVI_{max}$  values are shown for three 10-year moving windows. NDVI, Normalized Difference Vegetation Index

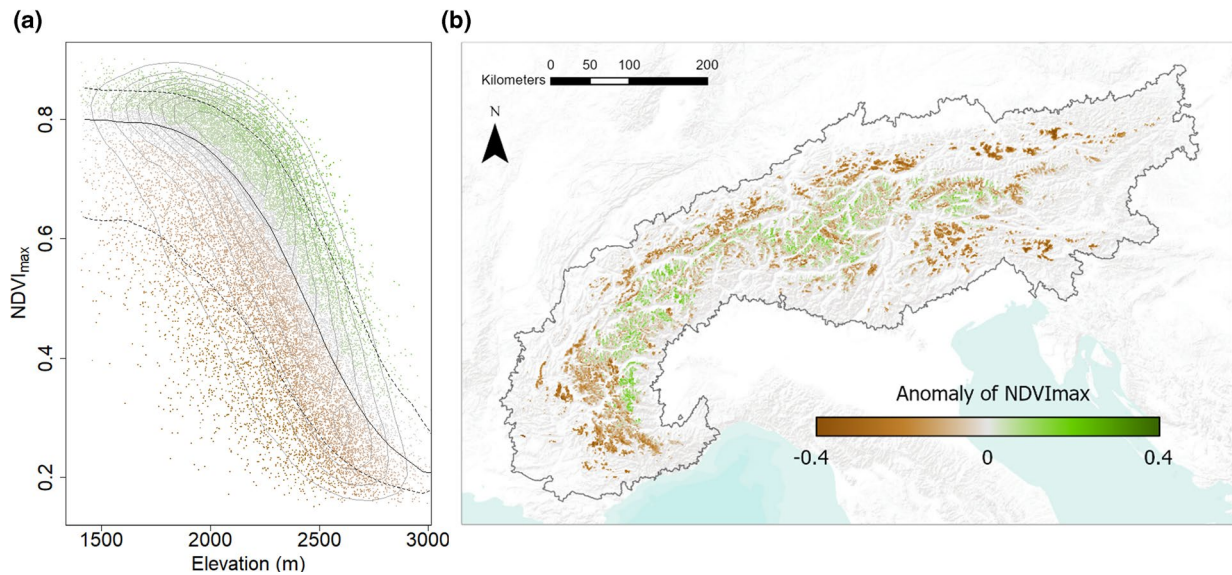


**FIGURE 4** Anomalies of  $NDVI_{max}$ . (a) An example of the variation of  $NDVI_{max}$  relative to elevation for DAH values in the  $-0.25$  to  $-0.2$  interval.  $NDVI_{max}$  values are averages for the 2000–2020 period. Black lines indicate the first, the fifth (median) and the ninth deciles of the distribution. The colour palette from brown to green expresses the  $NDVI_{max}$  anomaly, that is the difference between  $NDVI_{max}$  and the median value of the corresponding elevation  $\times$  DAH combination. (b) Spatial distribution of the  $NDVI_{max}$  anomaly in the European Alps. For visual clarity, we applied a  $5 \times 5$  moving window to the original 250-m resolution map. DAH, diurnal anisotropic heating; NDVI, Normalized Difference Vegetation Index

greening ( $p < .005$ ). The model classified the ‘no greening’ and the ‘fast greening’ classes with an accuracy of 61.5% and 62%, respectively, corresponding to a kappa of .42 and .4 (Table S3). The values of the first and ninth deciles of the 1000 simulations differ by  $<2\%$  from the mean. The performance of the random forest classifier for the ‘moderate greening’ was low with an overall accuracy of 0.51 to be compared to a random accuracy of 0.33 (Table S3).

The ranking of predictors shows that the  $NDVI_{max}$  anomaly is as important as climate predictors (Figure 5a,b). Noticeably, its score is high for both the mean decrease accuracy and the mean decrease in Gini coefficient, indicating a high suitability as a predictor and a high contribution to the homogeneity of nodes and leaves. By contrast, climate predictors show high decrease in permutation tests but do not exhibit a high contribution to the purity of nodes (low mean decrease in Gini), while topographical predictors show the reverse trend (Figure 5b). The greening trends did not change between bedrock types (Figure S5) and bedrock exhibited a very low variable importance in random forest. For these reasons, it was not retained in further analysis. Partial dependence plots (Figure 5c) reveal that greening was mostly associated with negative  $NDVI_{max}$  anomalies, negative DAH, elevation between 2300 and 2700 m and increasing green-up dates, and were marginally enhanced by a more positive trend in GDD and water balance. The lack of greening occurs more often at low and very high elevation, where  $NDVI_{max}$  anomaly was positive and green-up dates decrease and, to a lesser extent, where climate amelioration was weak (Figure 5c). Given the positive correlation between snow melt-out date and green-up date above treeline, our results indirectly point to a positive effect of delayed

snow melt on the recent greening trends. We also implemented complementary random forest models for subsets of pixels lying in narrower ranges of  $NDVI_{max}$  (0.15–0.4 and 0.4–0.65) and by adding  $NDVI_{max}$  as a supplementary predictor (Figure S6). The ranking of variable importance was consistent for all these simulations, which also confirmed the overwhelming importance of the  $NDVI_{max}$  anomaly for predicting the greening response whatever the  $NDVI_{max}$  value (Figure S6). They also pointed out that adding the  $NDVI_{max}$  as a supplementary predictor tends to lower the importance of the  $NDVI_{max}$  anomaly (Figure 5a; Figure S6a), which is explainable by the positive correlation between these two variables.

The strong link between negative  $NDVI_{max}$  anomalies and significant greening trends led us to explore at a finer scale the land cover features associated with these contexts. Using very high-resolution satellite imagery from Google Earth, we performed a visual photointerpretation of 300 randomly selected sites across the Alps (Figure S7). First, this analysis indicated that  $NDVI_{max}$  anomalies were consistently negative in the case of high cover of screes, debris and outcrops (Figure 6a). The reverse trend holds for grassland cover (Figure 6c). Second, the magnitude of greening tends to increase with the cover of screes and debris and decreases with that of grasslands (Figure 6b,d). Last, we did not find evidence that the presence of nearby trees or tall shrubs was associated with more frequent greening, suggesting that the densification of non-woody vegetation is as important as the upward shift of trees to explain greening. This is illustrated by four examples of land cover dynamics using past and current very high-resolution colour-infrared aerial photographs that are available for the French Alps (Figure S8).

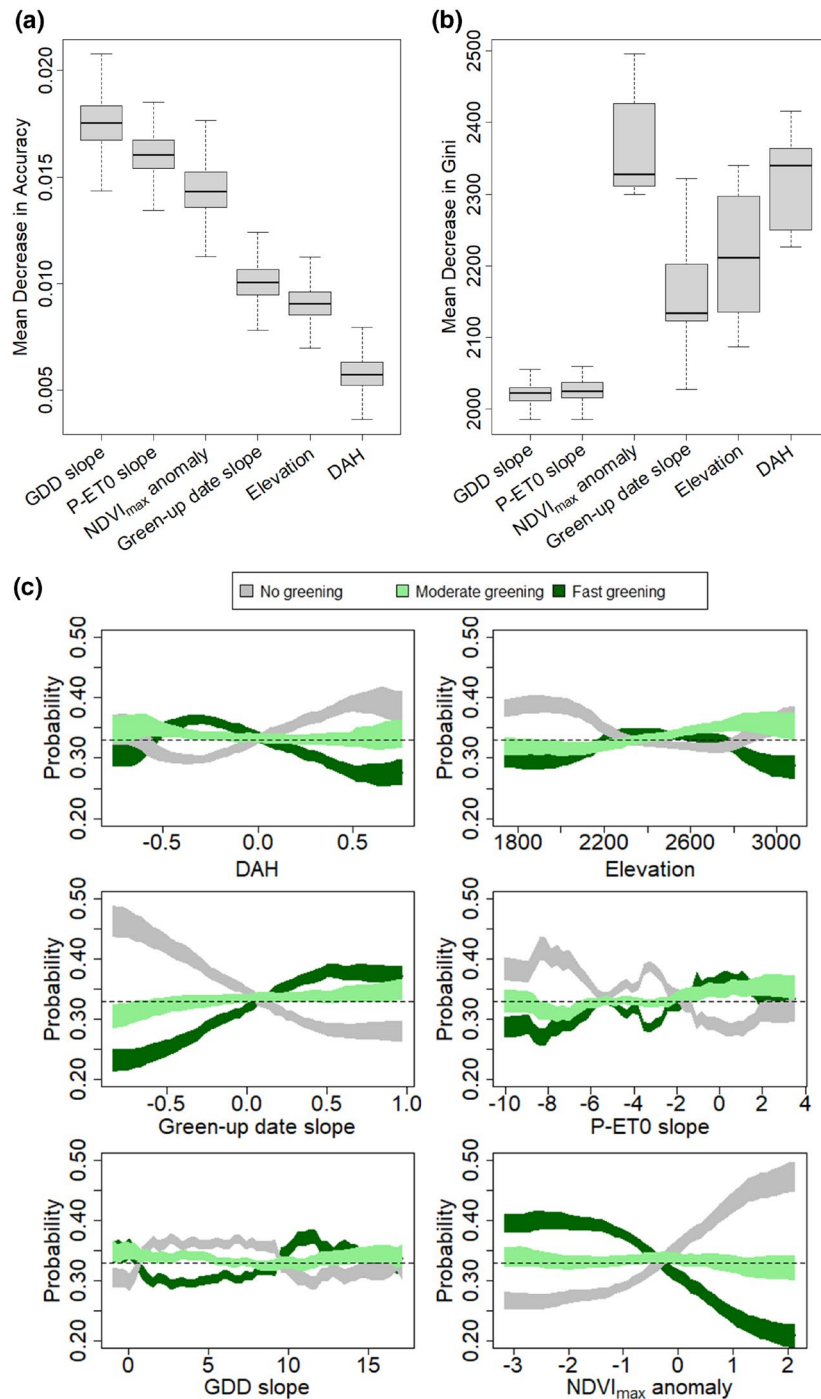


**FIGURE 5** Predictors of greenness trends. We classified pixels into three categories—no greening, moderate greening ( $.005 < p < .05$ ) and fast greening ( $p < .005$ )—and implemented a random forest model to assess the importance of predictors. (a) Predictor efficacy for classification measured by the mean accuracy decrease in classification following permutation of variables. (b) Contribution of a predictor to the purity of nodes measured by the decrease in the Gini coefficient. (c) Partial dependency analyses showing the classification probability as a function of the predictor values. We created 1000 perturbed data sets of MODIS reflectance for the 284,346 pixels and then randomly selected 30,000 pixels in each data set. These subsets of pixels were split into training (66%) and validation (33%) to implement the random forest model. Envelopes show the first and ninth deciles of the predicted distribution. DAH, diurnal anisotropic heating; GDD, growing degree days; NDVI, Normalized Difference Vegetation Index

## 4 | DISCUSSION

The main findings of our study are threefold. First, more than half of the land surface occupied by above-treeline ecosystems in the

European Alps has experienced significant greening over the last two decades. By contrast, the number of pixels showing significant browning trends is <1%. Second, this widespread greening is spatially non-uniform, and fast greening responses can be explained by a



combination of local-scale factors—that is, elevation and exposure—and regional-scale factors pertaining to anomalies of  $\text{NDVI}_{\text{max}}$  and trends in green-up dates. Third, we provided substantial evidence for the high responsiveness of north-facing and sparsely vegetated areas that have clearly benefited the most from recent climate changes in the European Alps.

Our study investigated greening trends across a vast and highly heterogeneous landscape. Above-treeline ecosystems in the Alps include a wide range of geomorphological, topographical and ecological situations that lead to a high turnover of plant communities over short distances. This fine-scale heterogeneity in plant cover inevitably calls into question the appropriateness of using moderate resolution remote sensing products to assess greening trends in mountainous landscapes. For example, it is entirely possible that contrasting trends in greenness are occurring within a 250-m resolution pixel because of habitat-specific responses (Matteodo et al., 2016). While the use of moderate resolution remote sensing products certainly limits our ability to assign specific  $\text{NDVI}_{\text{max}}$  trajectories to particular plant communities or habitats, our approach nonetheless provides a very valuable and comprehensive picture of vegetation shifts at the mountain range scale, and enables broad-scale investigation of land cover dynamics as demonstrated in previous studies (Zhao & Running, 2010). We acknowledge the potential of using high-resolution products such as the Landsat archive to complement our study. However, this will raise other difficulties. The most critical is the low frequency of available images, which makes it difficult to capture the peak of growth in alpine environments, and leads to large uncertainties in the estimate of  $\text{NDVI}_{\text{max}}$ . In addition, calculating a finer grained greening response would exacerbate the mismatch between the spatial scale of remote sensing products and that of drivers of changes, especially climate (Randin et al., 2020). For these reasons, we believe that high-resolution remote sensing data would be more appropriate to examine the responses of specific habitats or sites for which ground-truth datasets are available. Similarly, the utilization of aerial photograph archives has an enormous, yet largely unexplored, potential to relate very fine-grained land cover dynamics to observed greening trends (see illustrative examples in Figure S8).

Another difficulty of our comparative analysis of greening trends pertains to the wide range of vegetation cover that is included. It is well known that NDVI exhibits a non-linear response to aboveground biomass and plant cover, especially for planophilous canopies (Myneni & Williams, 1994). The sensitivity of NDVI to an incremental change in biomass or cover decreases for dense canopies, as does our capacity to detect a significant greenness trend in these contexts. Thus, one may run the risk that the spatial variability of greening partly reflects the different sensitivity of the method used to detect greening. We paid particular attention to this issue and removed from our analysis all pixels with high  $\text{NDVI}_{\text{max}}$  values ( $>0.65$ ), as we had clear indications of a saturation effect on greening (Figure S2). The relationship between  $\text{NDVI}_{\text{max}}$  and biomass or cover is linear in the  $\text{NDVI}_{\text{max}}$  range we selected (Myneni & Williams, 1994). We also performed similar random forest analyses on subsets

of pixels exhibiting very low  $\text{NDVI}_{\text{max}}$  value and found similar conclusions (Figure S6). For these reasons, we are confident that the saturation of  $\text{NDVI}_{\text{max}}$  with aboveground biomass did not blur our assessment of greening trends in the European Alps.

Our report on widespread greening in above-treeline ecosystems of the Alps is consistent with previous studies on arctic and alpine ecosystems (Berner et al., 2020; Ju & Masek, 2016; Krakauer et al., 2017; Xie et al., 2020). As in other cold parts of the Earth, high-elevation ecosystems in the Alps have experienced a more pronounced warming than lowlands (Palazzi et al., 2019; Pepin et al., 2015) and, not surprisingly, these temperature-limited ecosystems are benefitting from this increased temperature. However, and by comparison to a recent report from the Arctic (Berner et al., 2020), we found very few significant browning trends. A plausible explanation is that all regions of the Alps have experienced warmer summers, albeit to varying degrees, over the last decades (Figure S9). This led us to consider that, at least for the Alps, the knowledge gap is less about the detection of significant greening trends than it is about the causes of its spatial variability in a warmer climate. Our study provides new perspectives on this matter, given that we unravelled the pivotal role of the anomaly of  $\text{NDVI}_{\text{max}}$  to capture part of this greening complexity. Ecosystems exhibiting a lower  $\text{NDVI}_{\text{max}}$  than expected given the topography, that is a negative anomaly, have been the most responsive over the last two decades, and this is the reason why we observe today a reduced dispersion of  $\text{NDVI}_{\text{max}}$  values for a given elevation  $\times$  DAH compared to the years 2000 (Figure 4b) as well as reduced regional heterogeneity (Figure 2). We can refer to this trend as a *catching-up phenomenon*, and we assert that it is the most important facet of the ongoing greening in the Alps.

To further understand this phenomenon, we paid particular attention to land cover properties using high-resolution images. Clearly, the presence of very sparsely vegetated surfaces—such as scree, talus and outcrops—is a predisposing factor to negative anomalies and greening (Figure 6). In this regard, our findings extend to a broader scale conclusions that were drawn from more localized studies (Carlson et al., 2017). Increasing vegetation cover in initially sparsely vegetated areas has been documented through long-term surveys (Rixen et al., 2014; Steinbauer et al., 2018) and remote sensing (Carlson et al., 2017). Noticeably, several reports have underlined the preferential expansion of tall shrubs and trees on scree and debris compared to nearby grasslands. In addition to forest ingrowth caused by land-use abandonment, this upward shift of trees is the other dimension of tree expansion documented in the Alps (Gehrig-Fasel et al., 2007; Vittoz, Rulence, et al., 2008), and diffuse treelines can be highly responsive to climate warming (Harsch et al., 2009). Forest dynamics at the treeline have also been influenced by the constant decline in pastoralism and the related human activities due to the land abandonment since the Industrial Revolution (1850), making it difficult to disentangle climate influence and human impacts (Motta & Nola, 2001). In the southern part of the Alps, these dynamics occur well above the treeline, which is mainly constituted by the European larch (*Larix decidua* L.) and

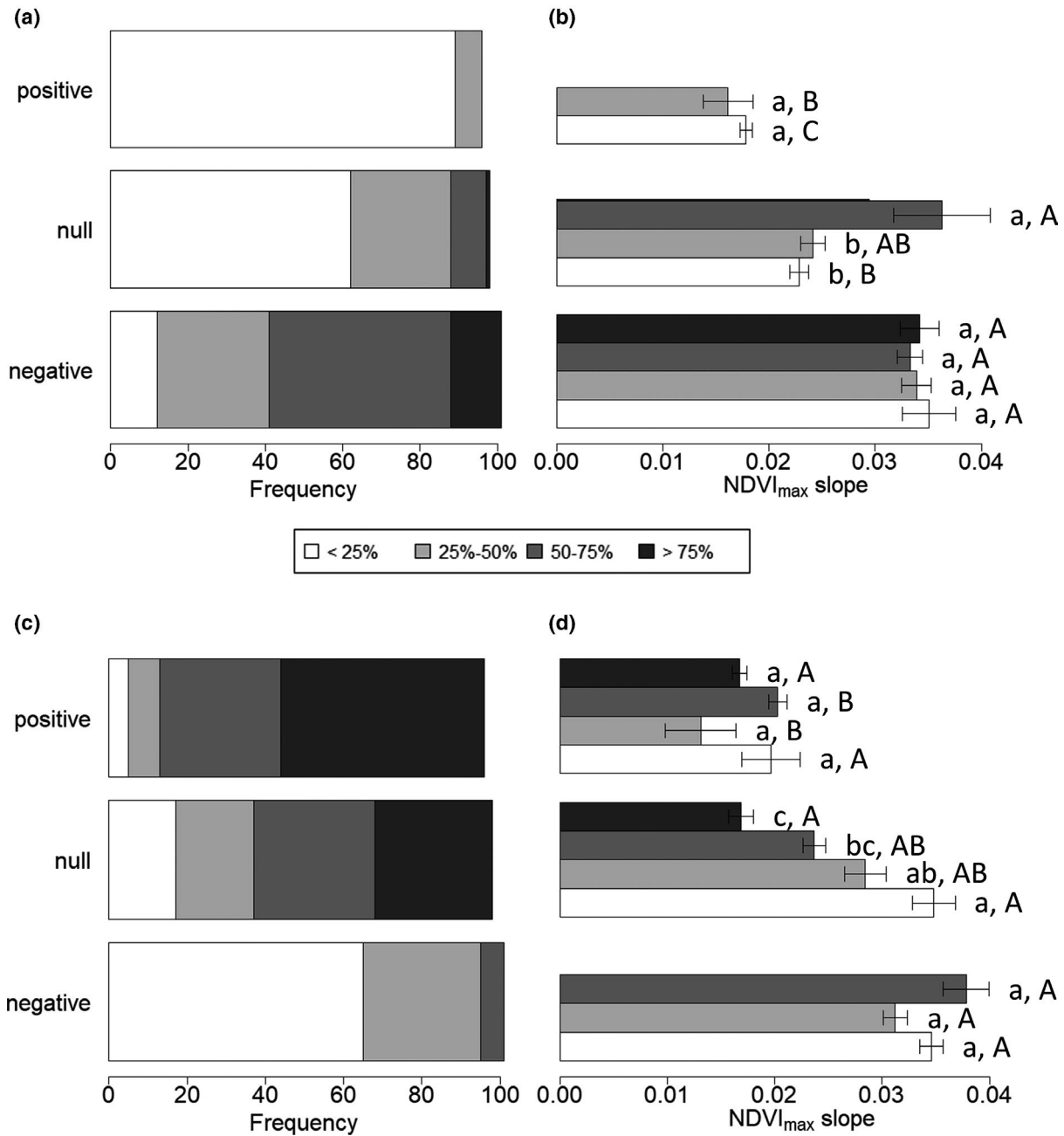


**FIGURE 6** Relationships between land cover, NDVI<sub>max</sub> anomalies and greenness trends. We randomly selected 100 pixels (500-m resolution) within three data subsets exhibiting negative, null and positive NDVI<sub>max</sub> anomalies (see Figure S7) and visually photointerpreted land cover using very high-resolution Google Earth imagery. Cover of screes/outcrops (a) and grasslands (b) per class of NDVI<sub>max</sub> anomaly. NDVI<sub>max</sub> slopes (mean ± SE) for each class of NDVI<sub>max</sub> anomaly distinguishing the cover of screes/outcrops (c) and grasslands (d). Results of a post hoc Tukey tests are denoted with letters. Different lower case letters indicate a significant ( $p < .05$ ) difference within NDVI<sub>max</sub> anomaly class. Different upper case letters indicate a significant ( $p < .05$ ) difference between NDVI<sub>max</sub> anomaly class. NDVI, Normalized Difference Vegetation Index

the stone pine (*P. cembra* L.). For example, the systematic survey of alpine ridges and cliffs in the south-western Alps led to the observation of isolated individuals or stands of *P. cembra* at very high elevation (e.g. >3000 m; André et al., 2020). This is consistent with the hypothesis that the upward shift of the treeline may be more pronounced in the inner part of the Alps where trees take advantage of the more continental, warmer and drier, climate (Körner, 1999).

Our study did not allow to precisely relate tree cover dynamics with greening because of the coarse resolution and the focus on high-elevation sites. Nonetheless, we noticed that the greening trends are more accentuated on north-facing slopes that are generally more forested and more densely covered by heathlands than southern aspects. Further studies should associate the different magnitudes of increase in NDVI<sub>max</sub> to well-documented colonization of

pioneer shrubs and trees. Our mapping of hotspots and coldspots of greening can provide the foundations for such an investigation coupling remote sensing and plant population models.

Another ecological dynamic that is consistent with our findings is the increasing cover of dwarf shrub—mainly *Ericaceous* species—in north-facing grasslands. Expanding low shrub cover in recent decades has been reported in the central Italian Alps at elevations up to 2500 m (Cannone et al., 2007). Coupled with climate change, the transition from an agro-pastoral socio-economic model to an economy based on tourism and skiing has enabled a pronounced expansion of trees and shrubs into mountain grasslands in numerous locations throughout the Alps since the 1950s, including, for example, the Chamonix valley (unpublished data). In addition to the expansion of woody vegetation, increasing grass cover in sparsely vegetated areas is probably contributing to the observed trends, both in the context of screes and talus as well as glacier forelands in the wake of glacier retreat (Mainetti et al., 2021).

Our study allowed for distinction between external drivers of greening such as climate and predisposing factors that pertain to the initial state of the responding system. Overall, the regional-scale variability of the greenness response did not strongly reflect spatial variation in climate change. Several reasons may explain this phenomenon. First, the climate data we used may be poor predictors because they fall short to capture surface conditions in high-elevation complex terrain. There are a limited number of weather stations above 2000 m in the Alps, and some variables like precipitation are notoriously difficult to model along topographical gradients (Frei & Isotta, 2019; Vionnet et al., 2019). Second, plant growth and community dynamics primarily respond to fine-scale thermal and moisture regimes that depend on landforms and soil factors (Giaccone et al., 2019; Liberati et al., 2019; Matteodo et al., 2016; Suding et al., 2015), and these factors are not accounted for in continental-scale gridded data sets. Third, high-elevation ecosystems may respond to different temporal scales of climate such as extreme events or past climate shifts. For example, previous studies have underlined the positive response of alpine primary productivity to heat waves (Corona-Lozada et al., 2019; Jolly et al., 2005). There is also strong evidence that the most significant rise of temperature in the Alps occurred in the late 1980s (EEA, 2009), that is a decade before the start of the MODIS observations. It is possible that these particularly favourable years lead to massive plant recruitment and that we are tracking the consequences of these events years later.

An example of a physical variable that we can track at the pixel scale is the green-up date, which strongly depends on the first snow free date. At first glance, our findings are counter-intuitive as the likelihood of greening is predominantly associated with a delayed green-up date (Figure 4), as illustrated by the situation in the south-western Alps and the south-central Alps (Figure S10). Using the regional climate re-analysis available for the French Alps, we confirmed that the positive trend for the green-up date is consistent with delayed snow melt-out during the last 20 years especially in the southernmost ranges and above 2000 m (Figure S11). A significant

decrease in snow melt-out dates in the 1980s and 1990s has been reported, mostly for sites below 2000 m (Durand et al., 2009; Klein et al., 2016; Matiu et al., 2021). Recent reports highlighted that these trends tend to vanish in the recent period, especially at high elevation (Matiu et al., 2021; Vorkauf et al., 2021). In line with these findings, there is evidence that high-elevation sites in the European Alps have experienced an increase in precipitation over the last decades (Avanzi et al., 2020; Napoli et al., 2019). We hypothesize that the combination of snowy winters and warm summers may be particularly favourable for alpine vegetation, especially where vacant niches are available for recruitment. This was suggested by Corona-Lozada et al. (2019) who showed that among the four main heat waves that hit the Alps in the last 20 years, the only one that did not translate into increased productivity was that of 2015 because a strong water deficit coincided with increased temperature. Recent work also indicated that earlier snow melt can be detrimental to the growth of *Rhododendron ferrugineum* shrubs that preferentially occur on north-facing slopes (Francon et al., 2020). It is therefore plausible that a delayed snow melt ameliorates the summer soil water balance and acts synergistically with warm summer temperatures to boost plant productivity and colonization, especially on north-facing slopes that may previously have been too cold to support dense vegetation cover. Further studies are needed to confirm that this association between prolonged snow cover and greening is not simply coincidental but is reflecting ecological mechanisms that are beneficial to plant recruitment and growth.

Finally, our findings call into question whether changes in pastoral management may have contributed to the negative  $NDVI_{max}$  anomalies and more generally to the contrasting regional greening trends. Unfortunately, consistent long-term data on mountain livestock systems are not available at the scale of the European Alps. A socio-economic analysis led Tappeiner et al. (2008) identified regions of the European Alps where agriculture has receded in recent years. Most of the Italian Alps and the North-easternmost Austrian Alps were described as 'forgotten rural areas' experiencing sharp declines in agriculture, which demonstrates substantial spatial consistencies with our delineation of greening hotspots. However, the analysis aggregated many different socio-economic variables at the scale of administrative districts, and it was not possible to include it in our analysis of the drivers of greening. There is certainly no simple relation between greening trends and changes in agricultural practices. For example, there has been a remarkable resilience of mountain livestock farming systems in the southern part of the French Alps, which is a greening hotspot, and this was observed despite many adverse factors such as demography, poor profitability, extreme events and return of the large predators (Hinojosa et al., 2016). Recent trends even point towards an increasing demand for high-elevation pastures to overcome the detrimental effects of droughts in lowlands and southernmost mountain ranges, leading shepherds to bring their flocks to high-elevation pastures for extended summer periods (Nettier et al., 2010). The greening trends we have documented here may further encourage such practices. This highlights that livestock farming systems cannot be solely envisaged as potential drivers of greening trends but that pastoral practices will also

have to adapt to the changing productivity and spatial distribution of mountain pastures (Jager et al., 2020).

## 5 | CONCLUSION

In summary, the uplands of the European Alps have undergone widespread albeit non-uniform greening over the last two decades. High-elevation ecosystems have positively responded to ongoing summer warming with varying degrees of sensitivity. This conclusion is supported by the importance of predisposing factors such as the NDVI<sub>max</sub> anomaly, that is an abnormally low initial greenness, which explains a substantial portion of the spatial variability of greening. Sparsely vegetated ecosystems on north-facing slopes and experiencing prolonged snow cover duration are the most highly responsive to ongoing warming, possibly because the positive effect of increased temperature is not dampened by limiting water supply and density-dependent plant competition. Our findings call for further studies examining why certain areas of the European Alps exhibit negative NDVI<sub>max</sub> anomalies and whether this determines specific ecological mechanisms underpinning observed greening trends.

## ACKNOWLEDGEMENTS

This work received funding from the LIFE PASTORALP Project (LIFE16 CCA/IT/000060) and the Interreg ALCOTRA CClimaTT. The authors acknowledge the E-OBS data set from the EU-FP6 project UERRA (<https://www.uerra.eu>), the Copernicus Climate Change Service and the data providers in the ECA&D project (<https://www.ecad.eu>). They are particularly grateful to the Parc National des Ecrins and the Parc National du Mercantour for their support and helpful discussions during the preparation of this work. Most of the computations presented in this paper were performed using the Froggy platform of the GRICAD infrastructure (<https://gricad.univ-grenoble-alpes.fr>), which is supported by the Rhône-Alpes region (GRANT CPER07\_13 CIRA), the OSUG@2020 labex (reference ANR10 LABX56) and the Equip@Meso Project (reference ANR-10-EQPX-29-01) of the Programme Investissements d'Avenir supervised by the Agence Nationale pour la Recherche. LECA is part of OSUG@2020 labex.

## CONFLICTS OF INTEREST

The authors declare that there is no conflict of interest.

## DATA AVAILABILITY STATEMENT

Data openly available in a public repository that issues datasets with DOIs.

## ORCID

Philippe Choler  <https://orcid.org/0000-0002-9062-2721>

Arthur Bayle  <https://orcid.org/0000-0002-3442-0789>

Bradley Z. Carlson  <https://orcid.org/0000-0002-5301-0494>

Christophe Randin  <https://orcid.org/0000-0002-4171-0178>

Gianluca Filippa  <https://orcid.org/0000-0002-4554-6045>

Edoardo Cremonese  <https://orcid.org/0000-0002-6708-8532>

## REFERENCES

- Anderson, K., Fawcett, D., Cugulliere, A., Benford, S., Jones, D., & Leng, R. L. (2020). Vegetation expansion in the subnival Hindu Kush Himalaya. *Global Change Biology*, 26(3), 1608–1625. <https://doi.org/10.1111/gcb.14919>
- André, G., Lavergne, S., & Carcaillet, C. (2020). *Unsuspected prevalent tree occurrences in high elevation sky-islands of the western Alps*. bioRxiv. <https://doi.org/10.1101/2020.07.08.193300>
- Asam, S., Callegari, M., Matiu, M., Fiore, G., De Gregorio, L., Jacob, A., Menzel, A., Zebisch, M., & Notarnicola, C. (2018). Relationship between spatiotemporal variations of climate, snow cover and plant phenology over the Alps—An Earth observation-based analysis. *Remote Sensing*, 10(11). <https://doi.org/10.3390/rs10111757>
- Avanzi, F., Ercolani, G., Gabellani, S., Cremonese, E., Pogliotti, P., Filippa, G., Morra di Cella, U., Ratto, S., Stevenin, H., Cauduro, M., & Juglair, S. (2020). Learning about precipitation lapse rates from snow course data improves water balance modeling. *Hydrology and Earth System Sciences*, 25(4), 2109–2131. <https://doi.org/10.5194/hess-25-2109-2021>
- Beniston, M. (2006). Mountain weather and climate: A general overview and a focus on climatic change in the Alps. *Hydrobiologia*, 562, 3–16. <https://doi.org/10.1007/s10750-005-1802-0>
- Berner, L. T., Massey, R., Jantz, P., Forbes, B. C., Macias-Fauria, M., Myers-Smith, I., Kumpula, T., Gauthier, G., Andreu-Hayles, L., Gaglioti, B. V., Burns, P., Zetterberg, P., D'Arrigo, R., & Goetz, S. J. (2020). Summer warming explains widespread but not uniform greening in the Arctic tundra biome. *Nature Communications*, 11(1). <https://doi.org/10.1038/s41467-020-18479-5>
- Böhner, J., & Antonić, O. (2009). Land-surface parameters specific to topo-climatology. *Developments in Soil Science*, 33, 195–226.
- Callaghan, T. V., Bergholm, F., Christensen, T. R., Jonasson, C., Kokfelt, U., & Johansson, M. (2010). A new climate era in the sub-Arctic: Accelerating climate changes and multiple impacts. *Geophysical Research Letters*, 37. <https://doi.org/10.1029/2009gl042064>
- Cannone, N., Sgorbati, S., & Guglielmin, M. (2007). Unexpected impacts of climate change on alpine vegetation. *Frontiers in Ecology and the Environment*, 5(7), 360–364. [https://doi.org/10.1890/1540-9295\(2007\)5\[360:UOCCO\]2.0.CO;2](https://doi.org/10.1890/1540-9295(2007)5[360:UOCCO]2.0.CO;2)
- Carlson, B. Z., Corona, M. C., Dentant, C., Bonet, R., Thuiller, W., & Choler, P. (2017). Observed long-term greening of alpine vegetation—a case study in the French Alps. *Environmental Research Letters*, 12(11). <https://doi.org/10.1088/1748-9326/aa84bd>
- Choler, P. (2015). Growth response of temperate mountain grasslands to inter-annual variations in snow cover duration. *Biogeosciences*, 12(12), 3885–3897. <https://doi.org/10.5194/bg-12-3885-2015>
- Cornes, R. C., van der Schrier, G., van den Besselaar, E. J. M., & Jones, P. D. (2018). An ensemble version of the E-OBS temperature and precipitation data sets. *Journal of Geophysical Research-Atmospheres*, 123(17), 9391–9409. <https://doi.org/10.1029/2017jd028200>
- Corona-Lozada, M. C., Morin, S., & Choler, P. (2019). Drought offsets the positive effect of summer heat waves on the canopy greenness of mountain grasslands. *Agricultural and Forest Meteorology*, 276. <https://doi.org/10.1016/j.agrformet.2019.107617>
- Cortés, J., Mahecha, M. D., Reichstein, M., Myneni, R. B., Chen, C., & Brenning, A. (2021). Where are global vegetation greening and browning trends significant? *Geophysical Research Letters*, 48(6), e2020GL091496. <https://doi.org/10.1029/2020GL091496>
- Dunn, A. H., & de Beurs, K. M. (2011). Land surface phenology of North American mountain environments using moderate resolution imaging spectroradiometer data. *Remote Sensing of Environment*, 115(5), 1220–1233. <https://doi.org/10.1016/j.rse.2011.01.005>
- Durand, Y., Giraud, G., Laternser, M., Etchevers, P., Mérindol, L., & Lesaffre, B. (2009). Reanalysis of 47 years of climate in the French Alps (1958–2005): Climatology and trends for snow cover. *Journal*

- of *Applied Meteorology and Climatology*, 48(12), 2487–2512. <https://doi.org/10.1175/2009jamc1810.1>
- Duveiller, G., Hooker, J., & Cescatti, A. (2018). The mark of vegetation change on Earth's surface energy balance. *Nature Communications*, 9. <https://doi.org/10.1038/s41467-017-02810-8>
- EEA. (2009). *Regional climate change adaptation. The Alps facing the challenge of changing water resources*. European Environment Agency.
- Filippa, G., Cremonese, E., Galvagno, M., Isabellon, M., Bayle, A., Choler, P., Carlson, B. Z., Gabellani, S., Morra di Cella, U., & Migliavacca, M. (2019). Climatic drivers of greening trends in the Alps. *Remote Sensing*, 11(21). <https://doi.org/10.3390/rs11212527>
- Fontana, F., Rixen, C., Jonas, T., Aberegg, G., & Wunderle, S. (2008). Alpine grassland phenology as seen in AVHRR, VEGETATION, and MODIS NDVI time series—A comparison with in situ measurements. *Sensors*, 8(4), 2833–2853. <https://doi.org/10.3390/s8042833>
- Forzieri, G., Alkama, R., Miralles, D. G., & Cescatti, A. (2017). Satellites reveal contrasting responses of regional climate to the widespread greening of Earth. *Science*, 356(6343), 1140–1144. <https://doi.org/10.1126/science.aal1727>
- Francon, L., Corona, C., Till-Bottraud, I., Choler, P., Carlson, B. Z., Charrier, G., Améglio, T., Morin, S., Eckert, N., Roussel, E., Lopez-Saez, J., & Stoffel, M. (2020). Assessing the effects of earlier snow melt-out on alpine shrub growth: The sooner the better? *Ecological Indicators*, 115. <https://doi.org/10.1016/j.ecolind.2020.106455>
- Frei, C., & Isotta, F. A. (2019). Ensemble spatial precipitation analysis from rain gauge data: Methodology and application in the European Alps. *Journal of Geophysical Research-Atmospheres*, 124(11), 5757–5778. <https://doi.org/10.1029/2018jd030004>
- Gehrig-Fasel, J., Guisan, A., & Zimmermann, N. E. (2007). Tree line shifts in the Swiss Alps: Climate change or land abandonment? *Journal of Vegetation Science*, 18(4), 571–582. <https://doi.org/10.1111/j.1654-1103.2007.tb02571.x>
- Giaccone, E., Luoto, M., Vittoz, P., Guisan, A., Mariethoz, G., & Lambiel, C. (2019). Influence of microclimate and geomorphological factors on alpine vegetation in the Western Swiss Alps. *Earth Surface Processes and Landforms*, 44(15), 3093–3107. <https://doi.org/10.1002/esp.4715>
- Gottfried, M., Pauli, H., Futschik, A., Akhalkatsi, M., Barančok, P., Benito Alonso, J. L., Coldea, G., Dick, J., Erschbamer, B., Fernández Calzado, M. R., Kazakis, G., Krajčí, J., Larsson, P., Mallaun, M., Michelsen, O., Moiseev, D., Moiseev, P., Molau, U., Merzouki, A., ... Grabherr, G. (2012). Continent-wide response of mountain vegetation to climate change. *Nature Climate Change*, 2(2), 111–115. <https://doi.org/10.1038/nclimate1329>
- Greenwell, B. M. (2017). pdp: An R package for constructing partial dependence plots. *The R Journal*, 9, 421–436. <https://doi.org/10.32614/RJ-2017-016>
- Hansen, S. (1984). Estimation of potential and actual evapotranspiration. *Nordic Hydrology*, 15(4–5), 205–212. <https://doi.org/10.2166/nh.1984.0017>
- Hantel, M., & Hirtl-Wielke, L. M. (2007). Sensitivity of Alpine snow cover to European temperature. *International Journal of Climatology*, 27(10), 1265–1275. <https://doi.org/10.1002/joc.1472>
- Harsch, M. A., Hulme, P. E., McGlone, M. S., & Duncan, R. P. (2009). Are treelines advancing? A global meta-analysis of treeline response to climate warming. *Ecology Letters*, 12(10), 1040–1049. <https://doi.org/10.1111/j.1461-0248.2009.01355.x>
- Hinojosa, L., Napoleone, C., Moulery, M., & Lambin, E. F. (2016). The "mountain effect" in the abandonment of grasslands: Insights from the French Southern Alps. *Agriculture Ecosystems & Environment*, 221, 115–124. <https://doi.org/10.1016/j.agee.2016.01.032>
- Hock, R., Rasul, G., Adler, C., Cáceres, B., Gruber, S., Hirabayashi, Y., Jackson, M., Kääb, A., Kang, S., Kutuzov, S., Milner, A., Molau, U., Morin, S., Orlove, B., & Steltzer, H. (2019). Chapter 2: High mountain areas. In H.-O. Pörtner, D. C. Roberts, V. Masson-Delmotte, P. Zhai, M. Tignor, E. Poloczanska, K. Mintenbeck, A. Alegría, M. Nicolai, A. Okem, J. Petzold, B. Rama, & N. M. Weyer (Eds.), *IPCC special report on ocean and cryosphere in a changing climate*. In press. <https://www.ipcc.ch/srocc/chapter/chapter-2/>
- Huete, A., Didan, K., Miura, T., Rodriguez, E. P., Gao, X., & Ferreira, L. G. (2002). Overview of the radiometric and biophysical performance of the MODIS vegetation indices. *Remote Sensing of Environment*, 83(1–2), 195–213. [https://doi.org/10.1016/s0034-4257\(02\)00096-2](https://doi.org/10.1016/s0034-4257(02)00096-2)
- Jager, H., Peratoner, G., Tappeiner, U., & Tasser, E. (2020). Grassland biomass balance in the European Alps: Current and future ecosystem service perspectives. *Ecosystem Services*, 45. <https://doi.org/10.1016/j.ecoser.2020.101163>
- Jolly, W. M., Dobbertin, M., Zimmermann, N. E., & Reichstein, M. (2005). Divergent vegetation growth responses to the 2003 heat wave in the Swiss Alps. *Geophysical Research Letters*, 32(18). <https://doi.org/10.1029/2005GL023252>
- Ju, J., & Masek, J. G. (2016). The vegetation greenness trend in Canada and US Alaska from 1984–2012 Landsat data. *Remote Sensing of Environment*, 176, 1–16. <https://doi.org/10.1016/j.rse.2016.01.001>
- Keenan, T. F., & Riley, W. J. (2018). Greening of the land surface in the world's cold regions consistent with recent warming. *Nature Climate Change*, 8(9), 825. <https://doi.org/10.1038/s41558-018-0258-y>
- Klein, G., Vitasse, Y., Rixen, C., Marty, C., & Rebetez, M. (2016). Shorter snow cover duration since 1970 in the Swiss Alps due to earlier snowmelt more than to later snow onset. *Climatic Change*, 139(3–4), 637–649. <https://doi.org/10.1007/s10584-016-1806-y>
- Körner, C. (1999). *Alpine plant life*. Springer Verlag.
- Krakauer, N. Y., Lakhankar, T., & Anadon, J. D. (2017). Mapping and attributing normalized difference vegetation index trends for Nepal. *Remote Sensing*, 9(10). <https://doi.org/10.3390/rs9100986>
- Kuhn, M. (2020). *Caret: Classification and regression training. R package version 6.0-86*. Retrieved from <https://CRAN.R-project.org/package=caret>
- Lamprecht, A., Semenchuk, P. R., Steinbauer, K., Winkler, M., & Pauli, H. (2018). Climate change leads to accelerated transformation of high-elevation vegetation in the central Alps. *New Phytologist*, 220(2), 447–459. <https://doi.org/10.1111/nph.15290>
- Liaw, A., & Wiener, M. (2002). Classification and regression by random Forest. *R News*, 2(3), 18–22.
- Liberati, L., Messerli, S., Matteodo, M., & Vittoz, P. (2019). Contrasting impacts of climate change on the vegetation of windy ridges and snowbeds in the Swiss Alps. *Alpine Botany*, 129(2), 95–105. <https://doi.org/10.1007/s00035-019-00223-5>
- Mainetti, A., D'Amico, M., Probo, M., Quaglia, E., Ravetto Enri, S., Celi, L., & Lonati, M. (2021). Successional herbaceous species affect soil processes in a high-elevation alpine proglacial chronosequence. *Frontiers in Environmental Science*, 8. <https://doi.org/10.3389/fenvs.2020.615499>
- Matiu, M., Crespi, A., Bertoldi, G., Carmagnola, C. M., Marty, C., Morin, S., Schöner, W., Cat Berro, D., Chiogna, G., De Gregorio, L., Kotlarski, S., Majone, B., Resch, G., Terzago, S., Valt, M., Beozzo, W., Cianfarra, P., Gouttevin, I., Marcolini, G., ... Weilguni, V. (2021). Observed snow depth trends in the European Alps: 1971 to 2019. *The Cryosphere*, 15(3), 1343–1382. <https://doi.org/10.5194/tc-15-1343-2021>
- Matteodo, M., Ammann, K., Verrecchia, E. P., & Vittoz, P. (2016). Snowbeds are more affected than other subalpine-alpine plant communities by climate change in the Swiss Alps. *Ecology and Evolution*, 6(19), 6969–6982. <https://doi.org/10.1002/ece3.2354>
- McLeod, A. I. (2005). *Kendall rank correlation and Mann-Kendall trend test. R package Version 2.2*. Retrieved from <https://CRAN.R-project.org/package=Kendall>
- Miura, T., Huete, A. R., & Yoshioka, H. (2000). Evaluation of sensor calibration uncertainties on vegetation indices for MODIS. *IEEE Transactions on Geoscience and Remote Sensing*, 38(3), 1399–1409. <https://doi.org/10.1109/36.843034>

- Motta, R., & Nola, P. (2001). Growth trends and dynamics in sub-alpine forest stands in the Varaita Valley (Piedmont, Italy) and their relationships with human activities and global change. *Journal of Vegetation Science*, 12(2), 219–230. <https://doi.org/10.2307/3236606>
- Myers-Smith, I. H., Kerby, J. T., Phoenix, G. K., Bjerke, J. W., Epstein, H. E., Assmann, J. J., John, C., Andreu-Hayles, L., Angers-Blondin, S., Beck, P. S. A., Berner, L. T., Bhatt, U. S., Bjorkman, A. D., Blok, D., Bryn, A., Christiansen, C. T., Cornelissen, J. H. C., Cunliffe, A. M., Elmendorf, S. C., ... Wipf, S. (2020). Complexity revealed in the greening of the Arctic. *Nature Climate Change*, 10(2), 106–117. <https://doi.org/10.1038/s41558-019-0688-1>
- Myneni, R. B., & Williams, D. L. (1994). On the relationship between FAPAR and NDVI. *Remote Sensing of Environment*, 49(3), 200–211. [https://doi.org/10.1016/0034-4257\(94\)90016-7](https://doi.org/10.1016/0034-4257(94)90016-7)
- Napoli, A., Crespi, A., Ragone, F., Maugeri, M., & Pasquero, C. (2019). Variability of orographic enhancement of precipitation in the Alpine region. *Scientific Reports*, 9, <https://doi.org/10.1038/s41598-019-49974-5>
- Nettier, B., Dobremez, L., Coussy, J.-L., & Romagny, T. (2010). Attitudes of livestock farmers and sensitivity of livestock farming systems to drought conditions in the French Alps. *Revue De Géographie Alpine-Journal of Alpine Research*, 98(1–4), 383–400. <https://doi.org/10.4000/rga.1307>
- Palazzi, E., Mortarini, L., Terzago, S., & von Hardenberg, J. (2019). Elevation-dependent warming in global climate model simulations at high spatial resolution. *Climate Dynamics*, 52(5–6), 2685–2702. <https://doi.org/10.1007/s00382-018-4287-z>
- Pepin, N., Bradley, R. S., Diaz, H. F., Baraer, M., Caceres, E. B., Forsythe, N., Fowler, H., Greenwood, G., Hashmi, M. Z., Liu, X. D., Miller, J. R., Ning, L., Ohmura, A., Palazzi, E., Rangwala, I., Schöner, W., Severskiy, I., Shahgedanova, M., Wang, M. B., ... Yang, D. Q. (2015). Elevation-dependent warming in mountain regions of the world. *Nature Climate Change*, 5(5), 424–430. <https://doi.org/10.1038/nclimate2563>
- Randin, C. F., Ashcroft, M. B., Bolliger, J., Cavender-Bares, J., Coops, N. C., Dullinger, S., Dirnböck, T., Eckert, S., Ellis, E., Fernández, N., Giuliani, G., Guisan, A., Jetz, W., Joost, S., Karger, D., Lembrechts, J., Lenoir, J., Luoto, M., Morin, X., ... Payne, D. (2020). Monitoring biodiversity in the Anthropocene using remote sensing in species distribution models. *Remote Sensing of Environment*, 239, <https://doi.org/10.1016/j.rse.2019.111626>
- Rixen, C., Wipf, S., Frei, E., & Stoeckli, V. (2014). Faster, higher, more? Past, present and future dynamics of alpine and arctic flora under climate change. *Alpine Botany*, 124(2), 77–79. <https://doi.org/10.1007/s00035-014-0141-z>
- Rogora, M., Frate, L., Carranza, M. L., Freppaz, M., Stanisci, A., Bertani, I., Bottarin, R., Brambilla, A., Canullo, R., Carbognani, M., Cerrato, C., Chelli, S., Cremonese, E., Cutini, M., Di Musciano, M., Erschbamer, B., Godone, D., Iocchi, M., Isabellon, M., ... Matteucci, G. (2018). Assessment of climate change effects on mountain ecosystems through a cross-site analysis in the Alps and Apennines. *Science of the Total Environment*, 624, 1429–1442. <https://doi.org/10.1016/j.scitotenv.2017.12.155>
- Ropars, P., & Boudreau, S. (2012). Shrub expansion at the forest-tundra ecotone: Spatial heterogeneity linked to local topography. *Environmental Research Letters*, 7(1), <https://doi.org/10.1088/1748-9326/7/1/015501>
- Ropars, P., Levesque, E., & Boudreau, S. (2015). Shrub densification heterogeneity in subarctic regions: The relative influence of historical and topographic variables. *Ecoscience*, 22(2–4), 83–95. <https://doi.org/10.1080/11956860.2015.1107262>
- Savitzky, A., & Golay, M. J. E. (1964). Smoothing and differentiation of data by simplified least squares procedures. *Analytical Chemistry*, 36, 1627–1639. <https://doi.org/10.1021/ac60214a047>
- Schoener, W., Koch, R., Matulla, C., Marty, C., & Tilg, A.-M. (2019). Spatiotemporal patterns of snow depth within the Swiss-Austrian Alps for the past half century (1961 to 2012) and linkages to climate change. *International Journal of Climatology*, 39(3), 1589–1603. <https://doi.org/10.1002/joc.5902>
- Signal Developers. (2013). *signal: Signal processing*. Retrieved from <http://r-forge.r-project.org/projects/signal/>
- Steinbauer, M. J., Grytnes, J.-A., Jurasinski, G., Kulonen, A., Lenoir, J., Pauli, H., Rixen, C., Winkler, M., Bardy-Durchhalter, M., Barni, E., Bjorkman, A. D., Breiner, F. T., Burg, S., Czortek, P., Dawes, M. A., Delimat, A., Dullinger, S., Erschbamer, B., Felde, V. A., ... Wipf, S. (2018). Accelerated increase in plant species richness on mountain summits is linked to warming. *Nature*, 556(7700), 231. <https://doi.org/10.1038/s41586-018-0005-6>
- Sturm, M., Schimel, J., Michaelson, G., Welker, J. M., Oberbauer, S. F., Liston, G. E., Fahnestock, J., & Romanovsky, V. E. (2005). Winter biological processes could help convert arctic tundra to shrubland. *BioScience*, 55(1), 17–26. [https://doi.org/10.1641/0006-3568\(2005\)055\[0017:wbpchc\]2.0.co;2](https://doi.org/10.1641/0006-3568(2005)055[0017:wbpchc]2.0.co;2)
- Suding, K. N., Farrer, E. C., King, A. J., Kueppers, L., & Spasojevic, M. J. (2015). Vegetation change at high elevation: Scale dependence and interactive effects on Niwot Ridge. *Plant Ecology & Diversity*, 8(5–6), 713–725. <https://doi.org/10.1080/17550874.2015.1010189>
- Tape, K. D., Hallinger, M., Welker, J. M., & Ruess, R. W. (2012). Landscape heterogeneity of shrub expansion in Arctic Alaska. *Ecosystems*, 15(5), 711–724. <https://doi.org/10.1007/s10021-012-9540-4>
- Tape, K. D., Sturm, M., & Racine, C. (2006). The evidence for shrub expansion in Northern Alaska and the Pan-Arctic. *Global Change Biology*, 12(4), 686–702. <https://doi.org/10.1111/j.1365-2486.2006.01128.x>
- Tappeiner, U., Borsdorf, A., & Tasser, E. (2008). *Mapping the Alps: Society–Economy–Environment*. Spektrum Akademischer Verlag.
- Tucker, C. J. (1979). Red and photographic infrared linear combinations for monitoring vegetation. *Remote Sensing of Environment*, 8(2), 127–150. [https://doi.org/10.1016/0034-4257\(79\)90013-0](https://doi.org/10.1016/0034-4257(79)90013-0)
- Venables, W., & Ripley, B. (2002). *Modern applied statistics* (S. Fourth, Ed.). Springer.
- Verbesselt, J., Hyndman, R., Newnham, G., & Culvenor, D. (2010). Detecting trend and seasonal changes in satellite image time series. *Remote Sensing of Environment*, 114(1), 106–115. <https://doi.org/10.1016/j.rse.2009.08.014>
- Vermote, E., & Vermeulen, A. (1999). *Atmospheric correction algorithm: Spectral reflectances (MOD09). ATBD version, 4, 1-107*. [https://eosps.gsf.nasa.gov/sites/default/files/atbd/atbd\\_mod08.pdf](https://eosps.gsf.nasa.gov/sites/default/files/atbd/atbd_mod08.pdf)
- Vernay, M., Lafaysse, M., Hagenmuller, P., Nheili, R., Verfaillie, D., & Morin, S. (2019). *The S2M meteorological and snow cover reanalysis in the French mountainous areas (1958–present)*. Dataset. <https://doi.org/10.25326/37>
- Vionnet, V., Six, D., Auger, L., Dumont, M., Lafaysse, M., Quéno, L., Réveillet, M., Dombrowski-Etchevers, I., Thibert, E., & Vincent, C. (2019). Sub-kilometer precipitation datasets for snowpack and glacier modeling in alpine terrain. *Frontiers in Earth Science*, 7, <https://doi.org/10.3389/feart.2019.00182>
- Viovy, N., Arino, O., & Belward, A. S. (1992). The Best Index Slope Extraction (BISE)—A method for reducing noise in NDVI time-series. *International Journal of Remote Sensing*, 13(8), 1585–1590. <https://doi.org/10.1080/01431169208904212>
- Vittoz, P., Bodin, J., Ungricht, S., Burga, C., & Walther, G. R. (2008). One century of vegetation change on Isla Persa, a nunatak in the Bernina massif in the Swiss Alps. *Journal of Vegetation Science*, 19(5), 671–628. <https://doi.org/10.3170/2008-8-18434>
- Vittoz, P., Rulence, B., Largey, T., & Frelechoux, F. (2008). Effects of climate and land-use change on the establishment and growth of cembra pine (*Pinus cembra* L.) over the altitudinal treeline ecotone in the

- Central Swiss Alps. *Arctic Antarctic and Alpine Research*, 40(1), 225–232. [https://doi.org/10.1657/1523-0430\(06-010\)\[vittoz\]2.0.co;2](https://doi.org/10.1657/1523-0430(06-010)[vittoz]2.0.co;2)
- Vorkauf, M., Marty, C., Kahmen, A., & Hiltbrunner, E. (2021). Past and future snowmelt trends in the Swiss Alps: The role of temperature and snowpack. *Climatic Change*, 165(3), 1–19.
- Xie, J., Jonas, T., Rixen, C., de Jong, R., Garonna, I., Notarnicola, C., Asam, S., Schaepman, M. E., & Kneubühler, M. (2020). Land surface phenology and greenness in Alpine grasslands driven by seasonal snow and meteorological factors. *Science of the Total Environment*, 725. <https://doi.org/10.1016/j.scitotenv.2020.138380>
- Zhang, G., Zhang, Y., Dong, J., & Xiao, X. (2013). Green-up dates in the Tibetan Plateau have continuously advanced from 1982 to 2011. *Proceedings of the National Academy of Sciences of the United States of America*, 110(11), 4309–4314. <https://doi.org/10.1073/pnas.1210423110>
- Zhao, M., & Running, S. W. (2010). Drought-induced reduction in global terrestrial net primary production from 2000 through 2009. *Science*, 329(5994), 940–943. <https://doi.org/10.1126/science.1192666>
- Zhu, Z., Piao, S., Myneni, R. B., Huang, M., Zeng, Z., Canadell, J. G., Ciais, P., Sitch, S., Friedlingstein, P., Arneth, A., Cao, C., Cheng,

L., Kato, E., Koven, C., Li, Y., Lian, X. U., Liu, Y., Liu, R., Mao, J., ... Zeng, N. (2016). Greening of the Earth and its drivers. *Nature Climate Change*, 6(8), 791. <https://doi.org/10.1038/nclimate3004>

## SUPPORTING INFORMATION

Additional supporting information may be found online in the Supporting Information section.

**How to cite this article:** Choler, P., Bayle, A., Carlson, B. Z., Randin, C., Filippa, G., & Cremonese, E. (2021). The tempo of greening in the European Alps: Spatial variations on a common theme. *Global Change Biology*, 00, 1–15. <https://doi.org/10.1111/gcb.15820>